



DNMI

Det norske meteorologiske institutt

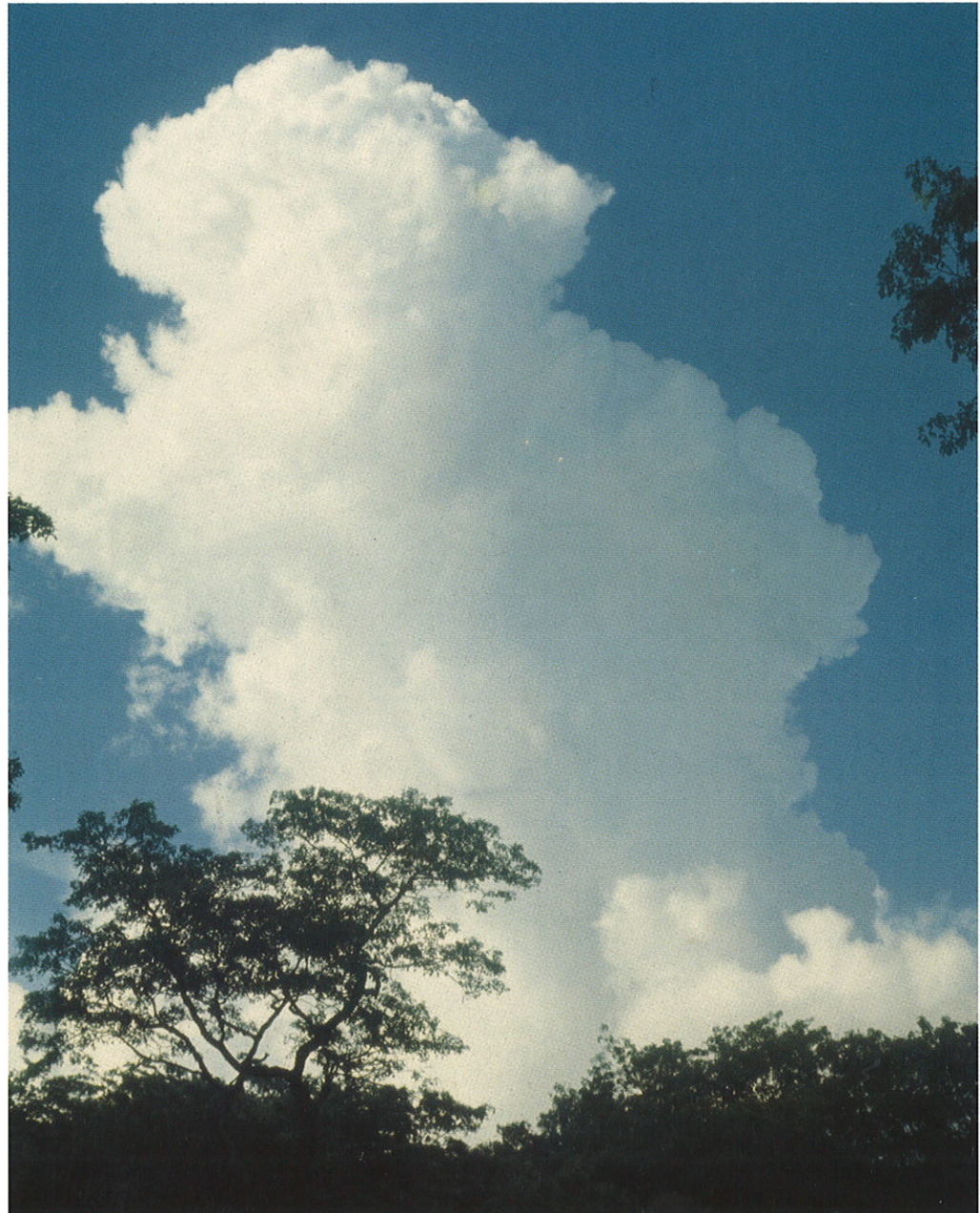
REPORT NO. 06/00

KLIMA

Reg Clim: Regional Climate Development
Under Global Warming

Evaluation and analysis of the
ECHAM4/OPYC3 GSDIO
temperature- and SLP-fields
over Norway and Svalbard.

Inger Hanssen-Bauer



DNMI – REPORT

ISSN 0805-9918

NORWEGIAN METEOROLOGICAL INSTITUTE
BOX 43 BLINDERN, N - 0313 OSLO

REPORT NO.
06/00 KLIMA

PHONE +47 22 96 30 00

DATE
08.02.00

TITLE

**Evaluation and analysis of the ECHAM4/OPYC3 GSDIO
temperature- and SLP-fields over Norway and Svalbard.**

AUTHOR

I. Hanssen-Bauer

PROJECT CONTRACTORS

Norwegian Research Council (Contracts No 120656/720&112890/720) and Norwegian Meteorological Institute

Abstract

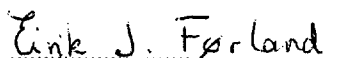
In the present report, monthly mean 2m temperatures (T) and sea level pressure (SLP) fields from the most recent integration (GSDIO) with the Max-Planck-Institute's global coupled climate model ECHAM4/OPYC3 are compared to the similar observed quantities over Norway and Svalbard. For temperature, values from selected grid-points are compared directly to values from selected stations. For SLP, modelled and observed gridded fields over the area 20°W-40°E and 50-85°N are compared by use of principal components referring to common EOFs. Finally, the connections between SLP fields and temperatures in Norway and at Svalbard deduced from historical data are compared to similar connections found in the results from the GSDIO integration.

The GSDIO "control climate" grid-point temperatures over Norway and Svalbard are in most cases found to be realistic, whenever it is possible to find stations with similar altitude and distance from coast. The GSDIO "future climate" indicates an annual mean warming of 0.2 - 0.5 °C/decade in the Norwegian grid-points, and 0.8 °C/decade in the Svalbard grid-point up to 2050. The warming is at maximum in winter, in the inland, and at high latitudes.

The GSDIO "control climate" SLP fields give at average a somewhat too weak westerly wind-field over Norway. The GSDIO "future climate" indicates an increase in the westerly wind component. Observations from the later decades show an increase in the westerly field of the same magnitude that is found in the GSDIO results during the same period.

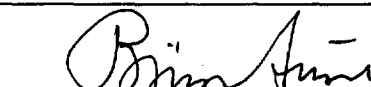
The observed connections between atmospheric circulation and temperatures in Norway and at Svalbard are satisfactorily reproduced in the GSDIO integration, especially in winter. The winter warming in the GSDIO integration may partly be explained by the increase in the westerly wind component. At the Norwegian mainland, a linear regression model based on atmospheric circulation indices accounts for 1/3 to 2/3 of the "scenario" warming in January. In July, the linear regression model does not account for any warming at all. The warming which is not accounted for by the linear regression model may be caused by non-linear processes including feedback mechanisms and air-sea-ice interactions, or it may be directly connected to changes in the climate forcing.

SIGNATURE



Eirik Førland

Principal Investigator, RegClim – PT 3



Bjørn Aune

Head of the Climatology Division

Evaluation and analysis of the ECHAM4/OPYC3 GSDIO temperature- and SLP-fields over Norway and Svalbard.

Foreword	4
1. Introduction	5
2. Data	6
3. Comparison of temperatures.....	8
3.1 Historical data vs. model data	8
3.2 Control temperatures vs. future temperatures	13
4. Comparison of SLP fields	16
4.1 Historical data vs. model data.....	16
4.2 Control SLP-fields vs. future SLP-fields.....	19
5. Comparison of connections between SLP-field and temperature.....	20
6. Conclusions	23
References	24
Appendix	25

FOREWORD

The present report is a result from the projects "Regional climate development under global warming" (Reg Clim) (Iversen et al. 1997) and "Long-term variations in atmospheric circulation and climate in the Norwegian Arctic", which both are supported by the Norwegian Research Council (NRC Contracts No 120656/720 and 112890/720).

1. Introduction

One of the aims for the Norwegian Reg Clim project (Regional Climate Development Under Global Warming) is to estimate probable changes in the regional climate in Norway, given a global warming. The project "Long-term variations in atmospheric circulation and climate in the Norwegian Arctic" aims at making similar estimates for Svalbard. In both projects, local future climate is, or will be, estimated by "downscaling" the results from global coupled atmosphere-ocean general circulation models (AOGCMs). The quality of estimates based upon any downscaling technique, strongly depends on the AOGCM's ability to realistically reproduce large-scale fields of variables, which can be used as predictors (in empirical downscaling) or boundary conditions (in dynamical downscaling). It is thus crucial to investigate whether the AOGCM on which the downscaling is based, is able to produce realistic large-scale fields of meteorological variables.

The "GSDIO" integration (a transient integration including greenhouse gases as well as direct and indirect sulphur aerosol forcing) with the Max-Planck-Institute's global coupled climate model ECHAM4/OPYC3 will be used as a basis for downscaling of future climate in Norway and on Svalbard (Figure 1). In the present report, results from the GSDIO integration will be compared to the similar observed quantities over Norway and Svalbard. Machenhauer et al. (1998) validated a number of different simulations over Europe, including 3 simulations with ECHAM4/OPYC3: A simulation of "present-day climate" (no changes of greenhouse gases), a GHG simulation (including increasing concentration of greenhouse gases) of historical climate (control climate), and a GHG simulation of future climate. Benestad et al. (1999) validated monthly fields from the ECHAM4/OPYC3 "present-day climate" simulation globally, but with focus on Scandinavia. Benestad (2000b) is carrying out a similar validation of the GSDIO integration. The aim of the present report is thus to study more in detail how the systematic errors of the GSDIO integration affect the large-scale atmospheric advection and the air temperatures over Norway and Svalbard.

The present report also includes comparisons between GSDIO control climate and future climate in these areas. The differences found in this way may serve as a "first guess" of the expected local climate changes. Further, it is of some interest to compare these changes to the differences between the GSDIO control climate and the observed climate. If the model's systematic errors exceed the expected climatic change, one should obviously use the results with care.

2. Data

Monthly sea level pressure (SLP) fields and 2 m air temperatures (T) from the GSDIO integration with ECHAM4/OPYC3 are used in the present study. The model-data were converted and quality controlled by Benestad (1999a). For T, a few grid-points were selected to represent the model data (Figure 1 and Table 1, column 1-4). Hanssen-Bauer and Nordli (1998) divided Norway into 6 temperature regions (Figure 1). In Table 1, the grid-points are identified by the number of the region they are taken to represent. Regions 2 and 4 are represented by two grid-points. The letters "s" (southern) and "n" (northern) are then used to distinguish between the points. Svalbard is defined as a separate region, denoted by "S".

To evaluate the realism of the model, mean values and standard deviations of observed and modelled monthly temperatures are compared. Data from selected Norwegian stations (Figure 1 and Table 1, column 5-8) are used. The stations are not necessarily as close as possible to the selected grid-points. An effort was made to find a station within the region the grid-point represents, with annual temperature amplitude similar to that of the grid-point. In Table 1, each station is given next to the grid-point to which it is compared in section 3.1.

Table 1. Geographical coordinates and height above sea level (m) for model grid-points and for stations.

Grid-point ID	Latitude (° N)	Longitude (° E)	Altitude (m)	Station	Latitude (degN)	Longitude (degE)	Altitude (m)
p1	59.5	11.2	327	Oslo	59.94	10.72	94
				Tryvann	59.99	10.69	528
				Sæli	59.33	8.25	655
p2s	59.5	5.6	252	Utsira	59.31	4.44	55
				Ulladal-F.	59.38	6.45	382
p2n	62.3	5.6	343	Ona	62.88	6.57	13
p3	62.3	11.2	501	Kjøbli	64.16	12.48	195
				Fokstua	62.11	9.29	972
p4s	65.1	14.1	433	Majavatn	65.18	13.42	339
p4n	70.6	22.5	65	Loppa	70.34	21.47	10
				Fruholmen	71.09	24.00	13
p5	67.8	25.3	360	Karasjok	69.47	25.51	129
				Suolovuopmi	69.59	23.53	374
p6	70.6	28.1	126	Vardø	70.37	31.08	14
				Sletnes Fyr	71.08	28.22	8
pS	78.9	16.9	106	Svalbard Airport	78.27	15.48	28

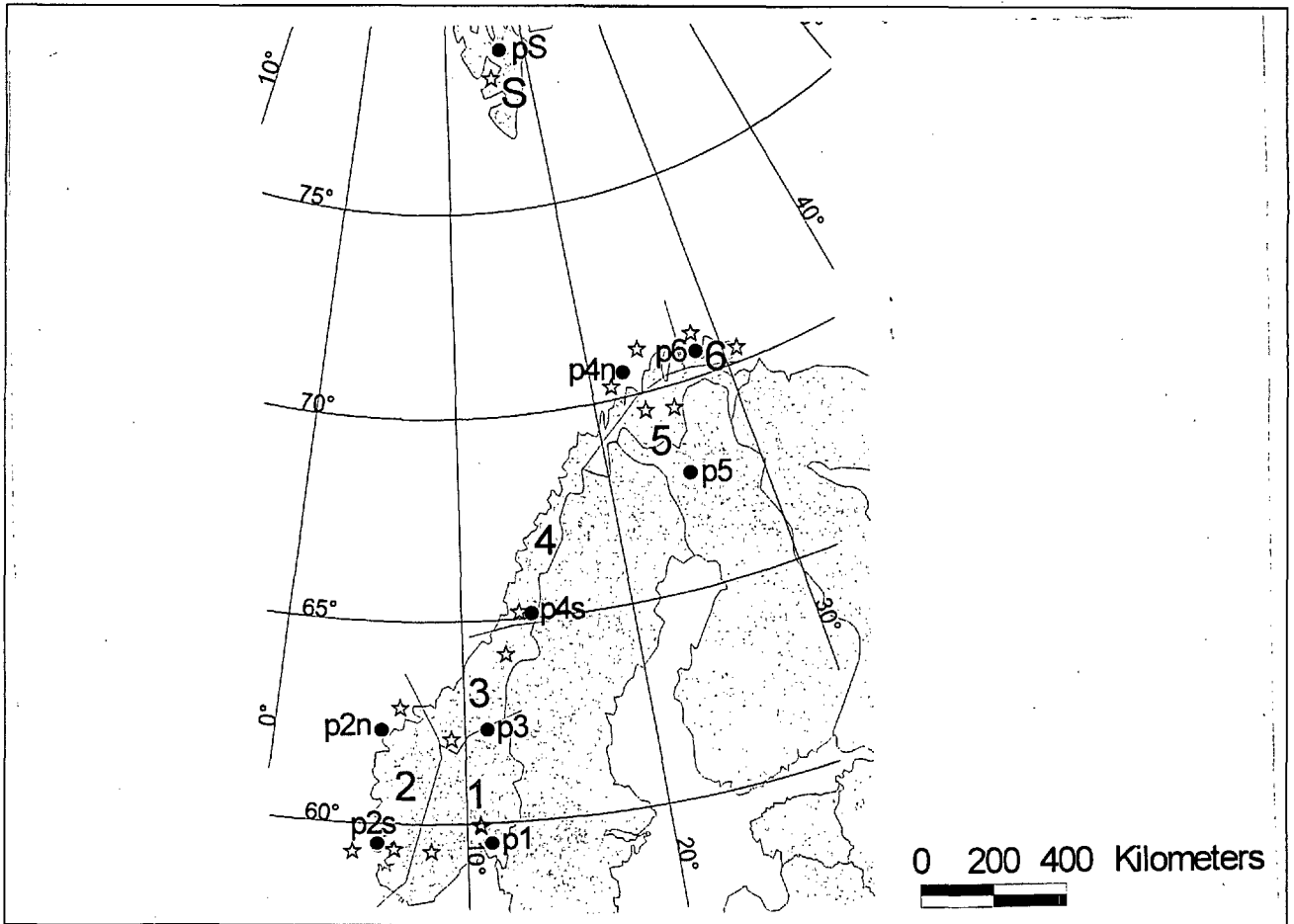


Figure 1. Temperature region 1-6, grid-points (•) and stations(☆) used in the temperature analyses.

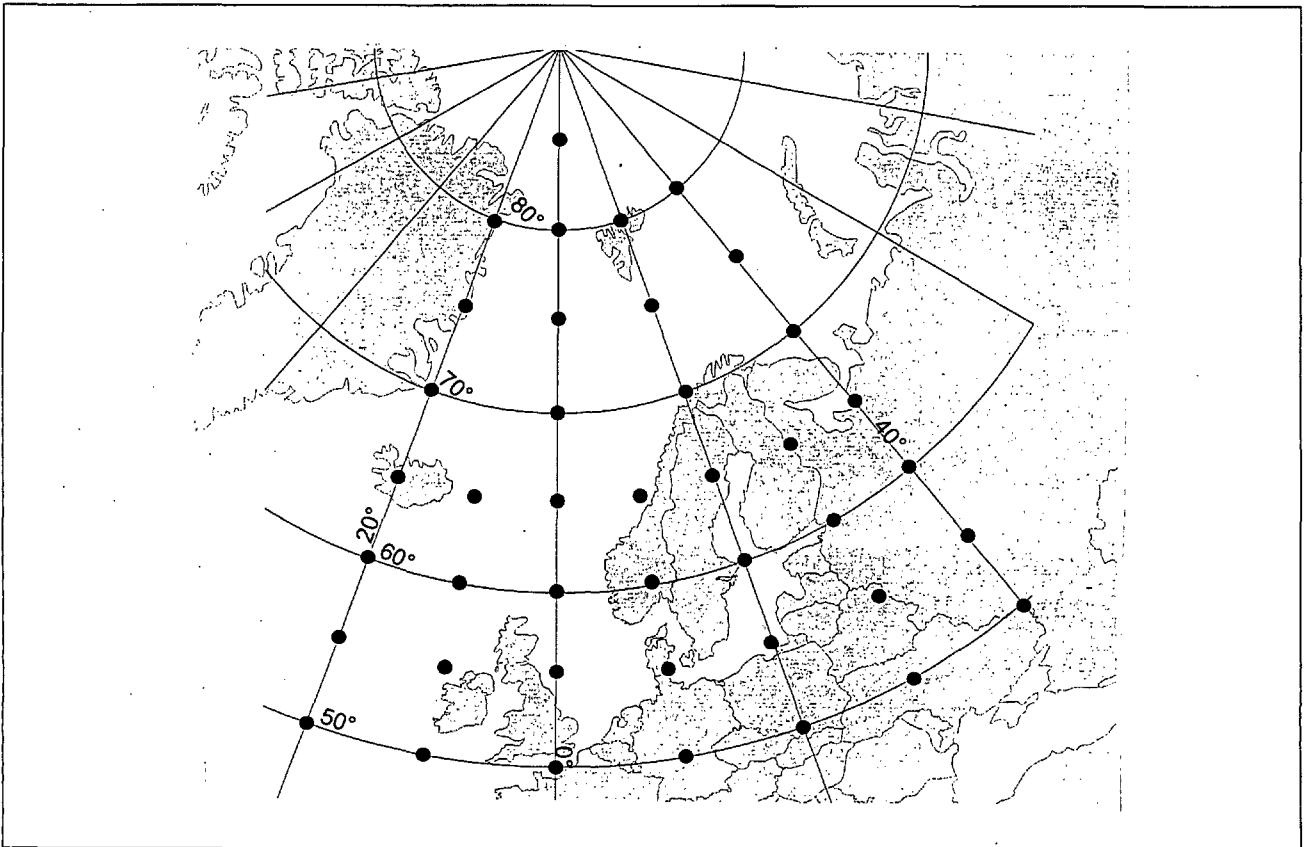


Figure 2. Grid-points used for SLP analyses.

For studying temperature trends and connections between atmospheric circulation and air temperature (section 5), regional series of standardised temperature for the 6 temperature regions shown in Figure 1 (Hanssen-Bauer and Nordli 1998) are used. Svalbard is represented by the standardised series from Svalbard Airport.

For SLP, model-data and observed data from the same grid-net within the area 20°W-40°E and 50-85 °N were used (Figure 2). The historical SLP data set used in the present study is a combination of the UK Met Office data-set and the NCEP data-set (Benestad 1998).

Modelled climate during the period 1860-1999, or during sub-periods within this period is referred to as “control climate”, while climate during the period 2000-2050 or within sub-periods of this is referred to as “future climate”.

3. Comparison of temperatures

3.1 Historical data vs. model data

Figure 3 shows the results from comparing monthly temperature averages and standard deviations from model grid-points to the similar values from climate stations in the same region. In the present comparison, one should not consider the modelled future climate (green curves and bars).

Grid-point 1 (Figure 3a, upper panel) was first compared to Oslo, which shows similar winter temperatures, but is considerably warmer in summer. This can at least partly be explained by the fact that the height above sea level for the Oslo station is lower than the model height at point 1 (Table 1). Comparisons of grid-point 1 with Tryvann and Sæli, which are situated higher above sea level, show very good correspondence. Note, however, that these stations are situated at least 200 m higher than the grid-point. The model temperatures in point 1 are thus somewhat lower than one might expect, except in winter. The grid-points in region 2 (Figure 3a middle and lower panels) are situated at the coast (Figure 1), and were thus both initially compared to lighthouse stations (Utsira and Ona). However, the altitudes of the model grid-points are considerably higher than the station altitudes (Table 1), thus it is hardly surprising that the modelled grid-point temperatures are considerably lower than the temperatures at the lighthouse stations. For grid-point 2n and Ona, the temperature difference is just what one might expect as the result from a height difference of 300-350m. For point 2s and Utsira, there is also a phase difference, probably because Utsira is a maritime station, while the grid-point is situated further inland in the model topography. Comparison of the temperature at grid-point 2s to the temperature at the near-by station Ulladal at about

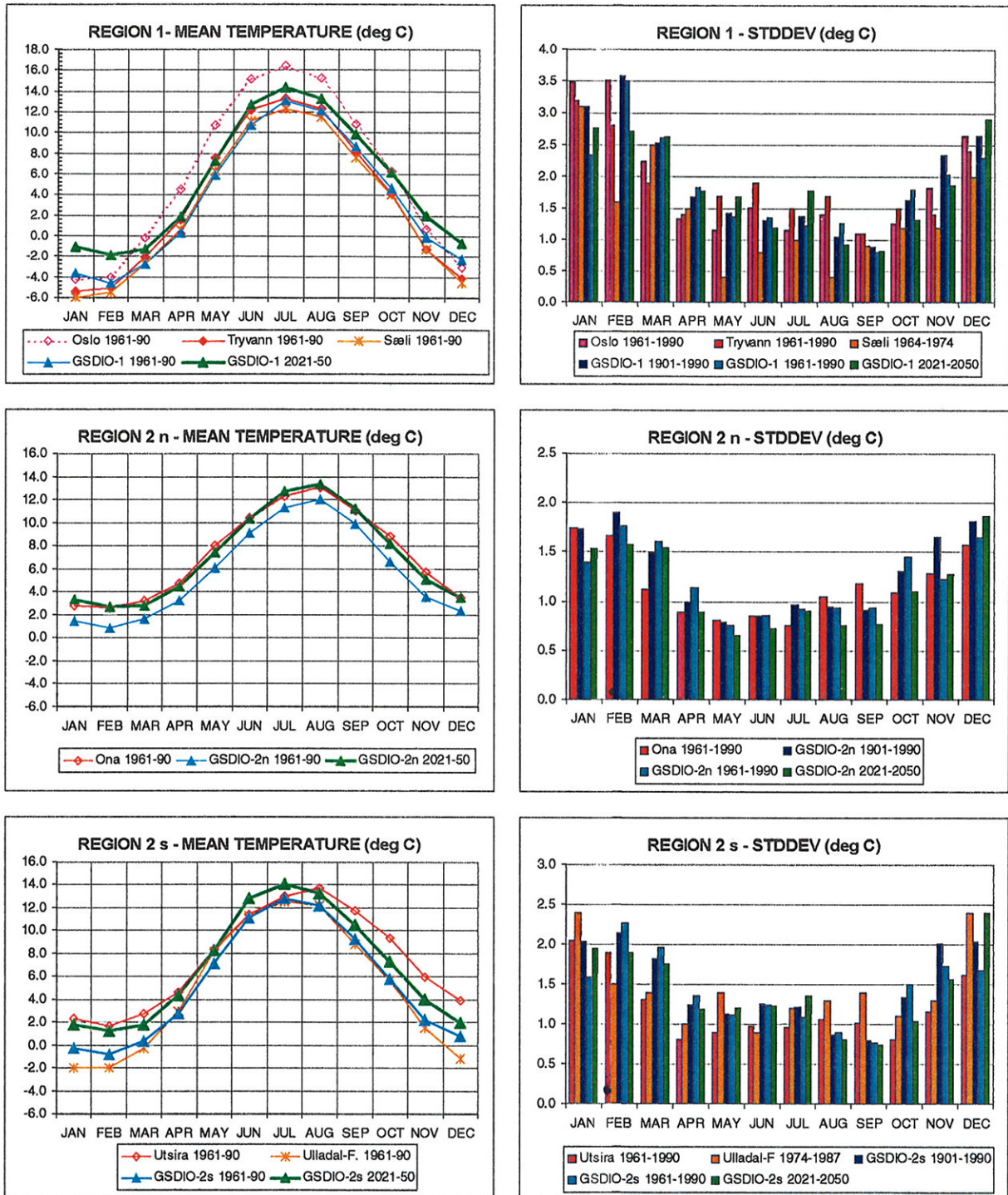


Figure 3a. Observed and modelled (GSDIO) monthly mean temperatures (left) and standard deviations of monthly mean temperatures (right) at selected grid-points and stations in temperature regions 1 and 2 (southern Norway). Red or orange curves/bars show values calculated from observations. Most of these are based on the period 1961-1990.

Blue or green curves/bars show values calculated from the model: Dark blue are based on model results for the period 1901-1990, cyanic on the period 1961-1990, while green are based on the period 2021-2050 (future scenario).

the same altitude and a bit inland from the coast shows good agreement, except in winter, when the modelled temperatures are somewhat higher than the observed ones. This can be caused by local ground inversions, which cannot be reproduced in the smooth model topography.

The temperatures in grid-point 3 (Figure 3b upper panel) are compared to the temperatures at one station situated about 300 m lower, and one situated almost 500 m higher. The grid-point temperature is quite close to the temperature of the lower station in summer, and most of the autumn and winter. These differences are smaller than one should expect from the height difference, probably because the station is quite a distance north of the grid-point. In spring, however, the grid-point temperatures are close to the temperatures of the more elevated station. Thus the model tends to be too cold in spring at this grid-point. The temperatures of the southernmost of the grid-points in region 4 (Figure 3b middle panel) are very close to the temperatures of near-by station Majavatn, which also is at about the same level a.s.l. But again, the model temperatures in spring tend to be somewhat lower than observed. This is also the case for the northernmost grid-point in region 4 (Figure 3b lower panel). At this grid point, the model temperatures in autumn, at the other hand, tend to be slightly too high.

The model temperature in grid-point 5 (Figure 3c, upper panel) is rather close to the station temperatures in region 5. In grid-point 6 (Figure 3c, middle panel), the model seems to be too warm in late summer and autumn. This is rather similar to the conditions in grid-point 4n. In both these grid-points, modelled monthly mean temperatures are clearly highest in August. It is possible to find stations where the August normal temperature is higher than the normal July temperature, but the temperature differences are then only some tenths of a degree.

The grid-point at Svalbard (Figure 3c, lower panel) is colder than the station Svalbard Airport except from the spring. The temperature difference, which is at maximum in winter (~ 5 °C), may only partly be explained by the height difference. It is probably more important that grid-point S in the model topography is farther from the coast than Svalbard Airport is in the real topography. But this makes it difficult to explain why spring-temperatures are close to those observed at this station.

The standard deviations of the monthly mean temperatures (Figure 3, right panels) seem to be rather realistically modelled in most cases. Most of the differences between model results and observation may be explained by differences concerning topography, marine influence, and length of time-series. Note the large differences between the period 1901-1990 and 1961-1990 concerning model standard deviations for the winter months for the grid-points 4n and 6. This is caused by two out-layers in the 1930s (see section 3.2), and the values for 1961-1990 are probably more realistic than the 1901-1990 values in these cases.

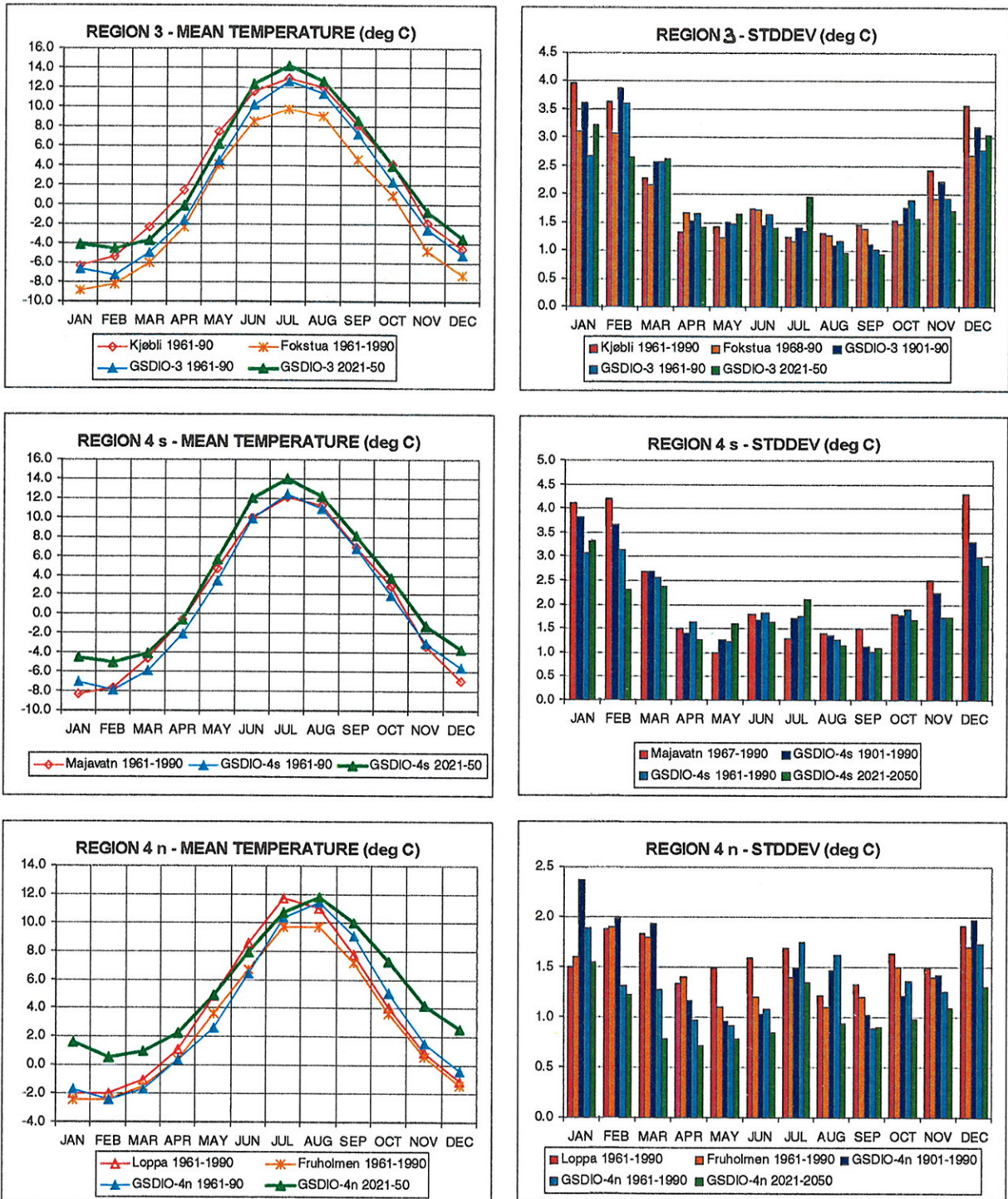


Figure 3b. Observed and modelled (GSDIO) monthly mean temperatures (left) and standard deviations of monthly mean temperatures (right) at selected grid-points and stations in temperature regions 3 and 4 (central and north-western Norway). Red or orange curves/bars show values calculated from observations. Most of these are based on the period 1961-1990. Blue or green curves/bars show values calculated from the model: Dark blue are based on model results for the period 1901-1990, cyanic on the period 1961-1990, while green are based on the period 2021-2050 (future scenario).

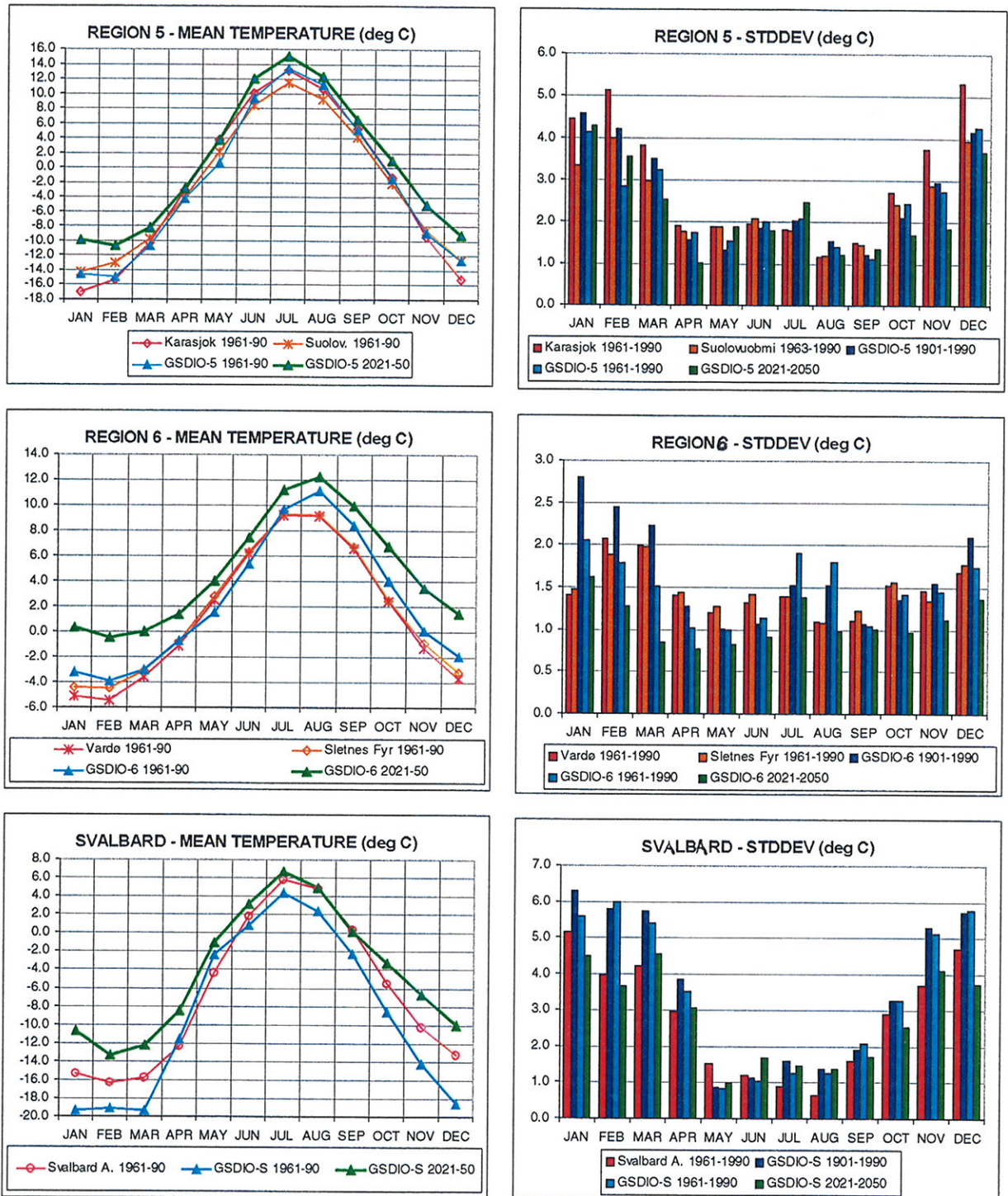


Figure 3c. Observed and modelled (GSDIO) monthly mean temperatures (left) and standard deviations of monthly mean temperatures (right) at selected grid-points and stations in temperature regions 5 and 6 (northern Norway) and Svalbard. Red or orange curves/bars show values calculated from observations. Most of these are based on the period 1961-1990. Blue or green curves/bars show values calculated from the model: Dark blue are based on model results for the period 1901-1990, cyanic on the period 1961-1990, while green are based on the period 2021-2050 (future scenario).

The above comparisons did not reveal large systematic errors in the model temperatures. In winter, the model gives too high temperatures at some locations, as it cannot simulate local ground inversions and cold-air pools caused by topographic features that are not resolved in the model topography. Further, data from coastal locations in mid- and north Norway may indicate a small seasonal shift in the model compared to observations: Model spring temperatures tend to be slightly too low and/or autumn temperatures slightly too high. However, this might be caused by differences between the model grid-points and stations concerning exposure for maritime air masses.

We conclude that the grid-point monthly temperatures in most cases reflect a climatology that is rather close to the observed climatology at near-by stations, provided that stations are found at the same altitude, and approximately at the same distance from the coast. It is thus important to know the model topography when interpreting model results from single grid-points.

3.2 Control temperatures vs. future temperatures

Differences between the model temperatures during the two 30-year periods 1961-1990 and 2021-2050 for each grid-point are seen from Figure 3, by comparing the blue and the green curves/bars. The warming tends to be larger in winter than in summer, larger at high latitudes than at low latitudes, and larger in the inland than at the coast. This is also seen when comparing the warming per decade from 1961-1990 to 2021-2050 for different grid-points and seasons (Figure 4). The fastest warming (almost 1.3 °C per decade) is found at Svalbard in winter (Dec-Jan-Feb). At the Norwegian mainland, the grid-point representing the northern inland (p5) shows the fastest warming (0.7 °C per decade), while the winter temperatures in grid-points 2s and 2n at the west coast increase by less than 0.3 °C per decade. In summer, the model shows a more uniform warming of about 0.2 °C per decade in most of the grid-points. The slowest warming is modelled in summer at the northern coast of Norway.

It is of some interest to know how large differences between two 30-year periods one might expect as the result from random variability. Averages and standard deviations based on monthly temperatures from the GSDIO integration were thus calculated for the six 30-year periods from 1870 to 2050. The maximum difference between the three first 30-year averages is largest (~3 °C) at Svalbard in January, but in all grid-points, the difference between the 2020-2050 average and the warmest of the three first 30-year averages is larger than the maximum difference between the first 3 (Figure 5, left panels). Thus, the temperature increase towards the last 30-year period is clearly larger than the random variation between different 30-year periods.

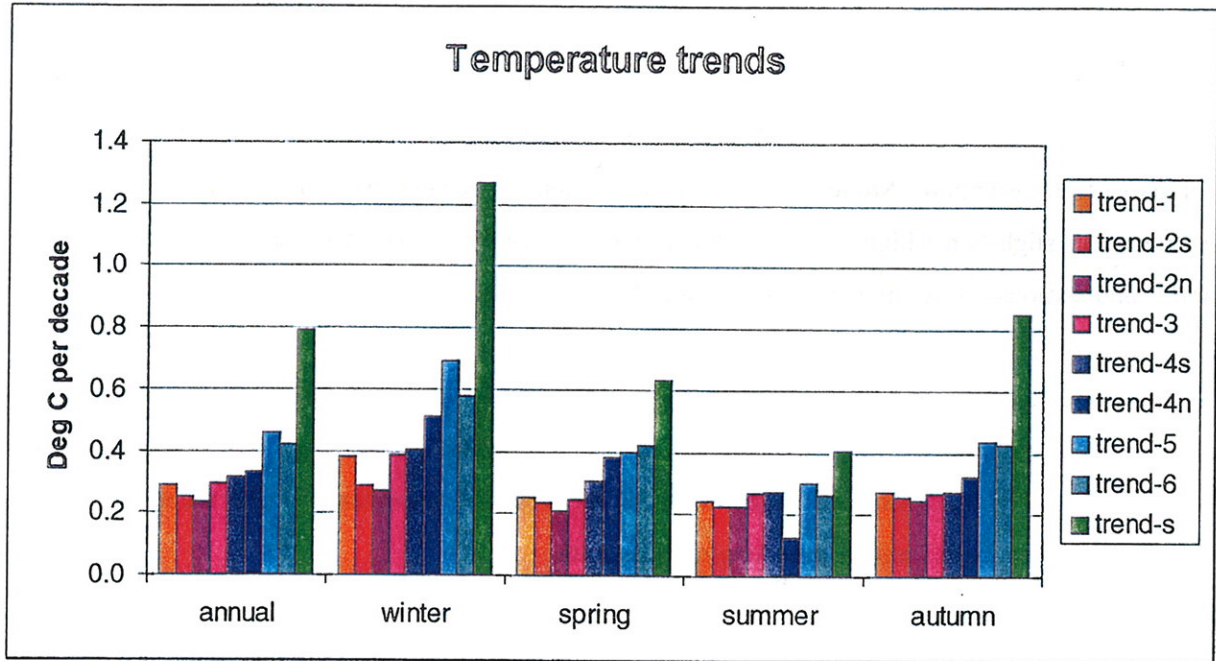


Figure 4. Temperature trends from GSDIO integration from the period 1961-1990 to the period 2020-2050. Trends are given for the grid-points shown in Fig.1. They are given on annual basis and for winter (Dec-Jan-Feb), spring (Mar-Apr-May), summer (Jun-Jul-Aug) and autumn (Sep-Oct-Nov).

Concerning monthly standard deviation (Figure 5, right panels) the grid-points at the northern coast (p4n and p6) show high values for January during the period 1931-1960 compared to the other periods. Extremely low January temperatures in 1932 and 1933, probably because sea ice has evolved too far south and west in the model, cause these large standard deviations. Except from this unrealistic variation in standard deviations, there seem to be no systematic variation in January standard deviations at the coastal grid-points (p2n, p4n and p6). However, the inland grid-points (p1, p3 and p5) as well as the grid-point at Svalbard tend to show lower values for the last three 30-year periods than for the first three in January. At Svalbard, this is also the case in April. At the Norwegian mainland, no systematic differences are found in the other seasons. The conclusion is that the GSDIO integration indicates less inter-annual variation in winter temperatures in the Norwegian inland, while the variation in other seasonal temperatures seem to be more or less unchanged. At Svalbard, the GSDIO integration indicates that the inter-annual variations in both winter and spring temperatures will decrease.

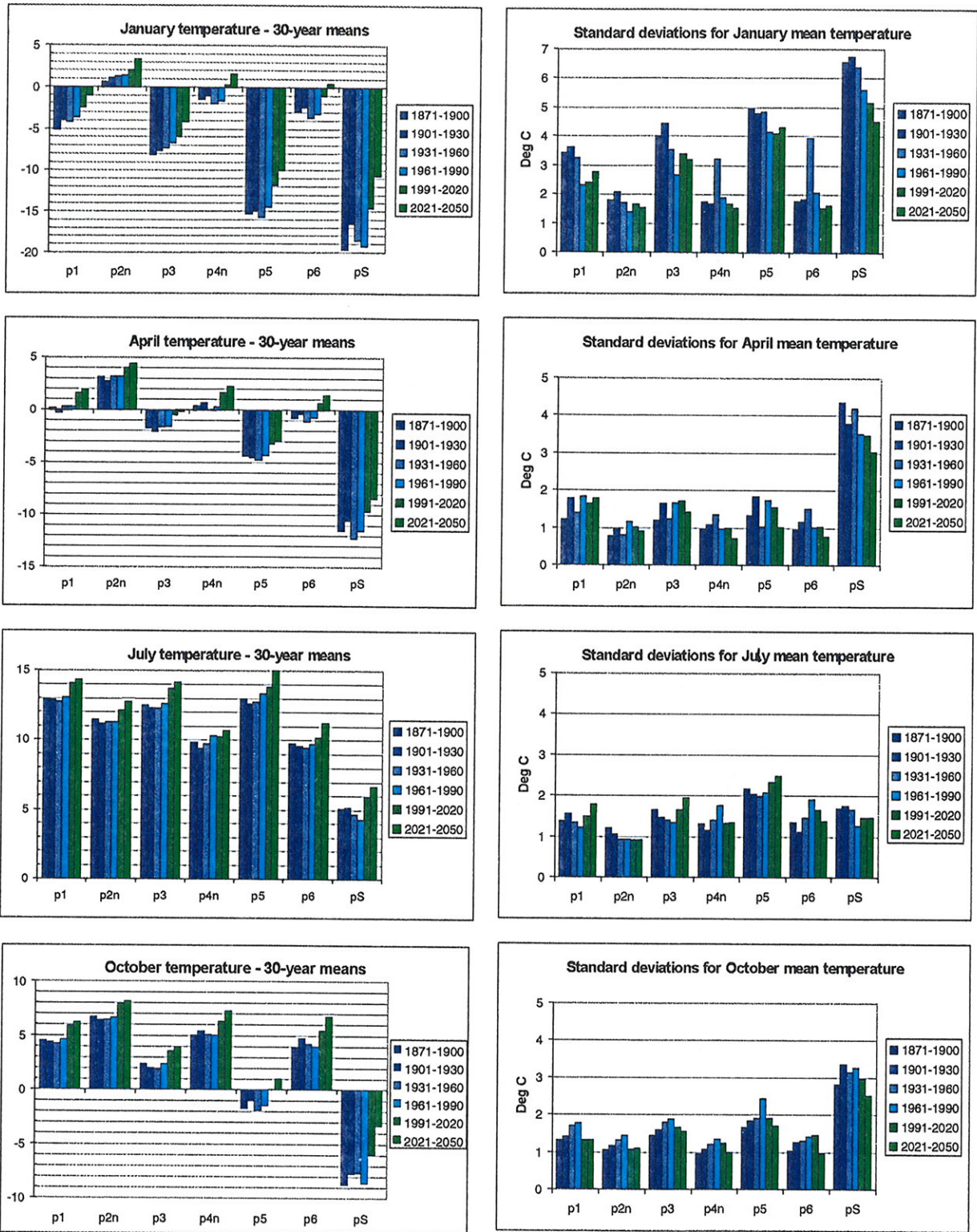


Figure 5. Modelled (GSDIO integration) 30-year mean temperature (left) and temperature standard deviation (right) at 7 grid-points for January, April, July and October.

4. Comparison of SLP-fields

4.1 Historical data vs. model data

For comparing observed and modelled SLP-fields, common EOFs (Benestad 1999b) were developed from observations during the period 1901-1997 and model results from the GSDIO integration during the period 1871-2050. The observed and modelled SLP-fields were combined without removing the mean values of each set first, as a main purpose of the present analysis is to compare observations and model and reveal systematic differences. The EOF analysis was accomplished using the SAS software procedure PRINCOMP (SAS Institute Inc. 1988). Eigenvalues and proportion of the variance accounted for by the 12 first EOFs are given in Table 2. The spatial patterns associated with the first 4 EOFs are given in Figure 6. The first 2 EOFs mainly include anomalies in the east-west component of the airflow over Norway, while the third and the fourth mainly include anomalies in the south-north component of this airflow.

Table 2. Eigenvalues of the Covariance Matrix in the common EOF analysis

	Eigenvalue	Difference	Proportion	Cumulative
EOF 1	593.63	285.21	0.419	0.419
EOF 2	308.42	40.31	0.218	0.637
EOF 3	268.12	191.39	0.189	0.826
EOF 4	76.73	11.87	0.054	0.880
EOF 5	64.86	23.06	0.046	0.926
EOF 6	41.81	29.16	0.030	0.956
EOF 7	12.65	1.65	0.009	0.965
EOF 8	11.00	2.09	0.008	0.973
EOF 9	8.91	2.85	0.006	0.979
EOF 10	6.07	2.29	0.004	0.983
EOF 11	3.78	0.61	0.003	0.986
EOF 12	3.17	0.18	0.002	0.988

Averaging the observed and modelled amplitude function (EOF scores) over succeeding 30-year periods (Figure 7a) gives an impression of eventual systematic errors of the modelled SLP fields over Norway. Systematic differences between model and observations are most pronounced for the first, the third, and the fourth EOF. The observations show at average negative score on the first EOF, while the GSDIO integration at average show a positive score. A negative score on the first EOF is associated with a positive anomaly in the westerly airflow over Norway and vice versa (Figure 6a). This implies that the average westerly wind-field over Norway produced by the GSDIO integration is somewhat too weak. This is in accordance with the conclusions drawn by Benestad et al. (1999) concerning the "greenhouse-gas integration" with the same model (ECHAM4/OPYC3).

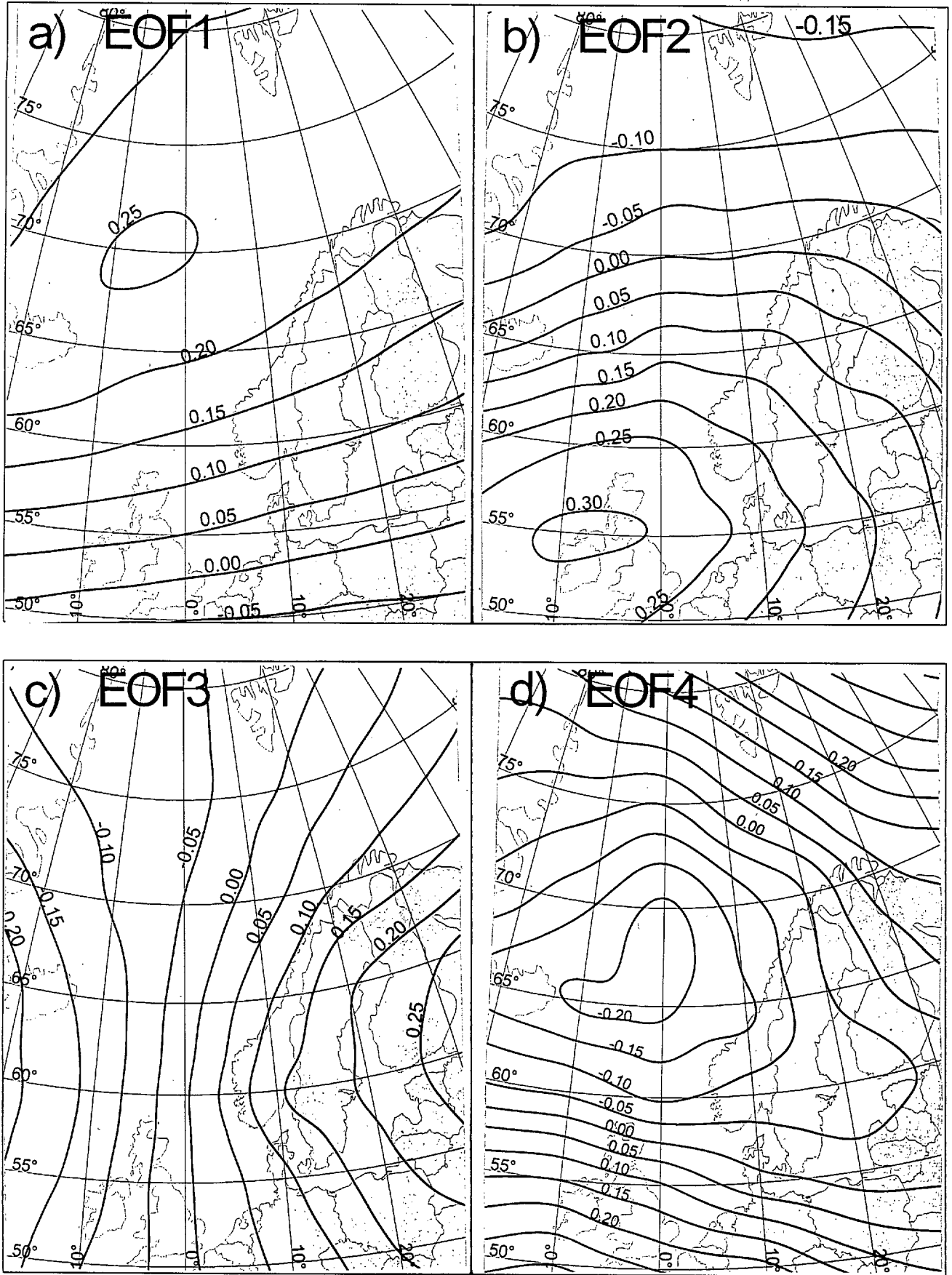
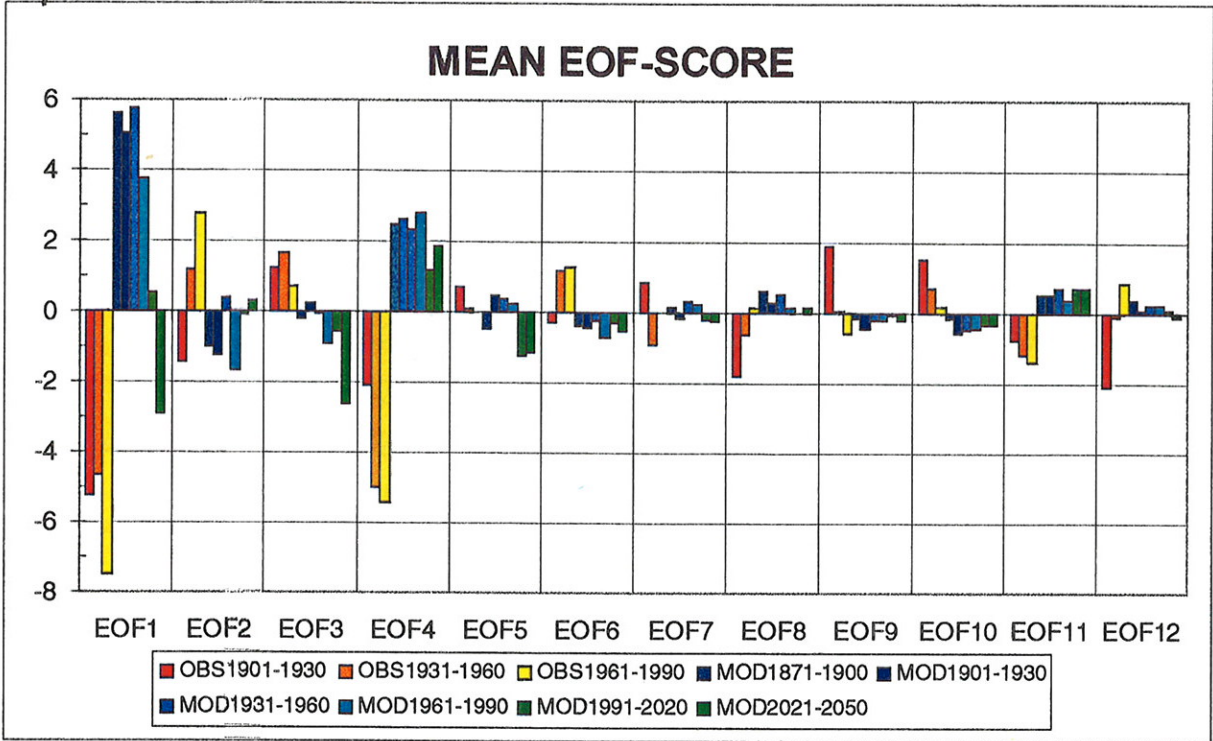


Figure 6. Spatial patterns associated with the first 4 common EOFs deduced from the SLP field.

a)



b)

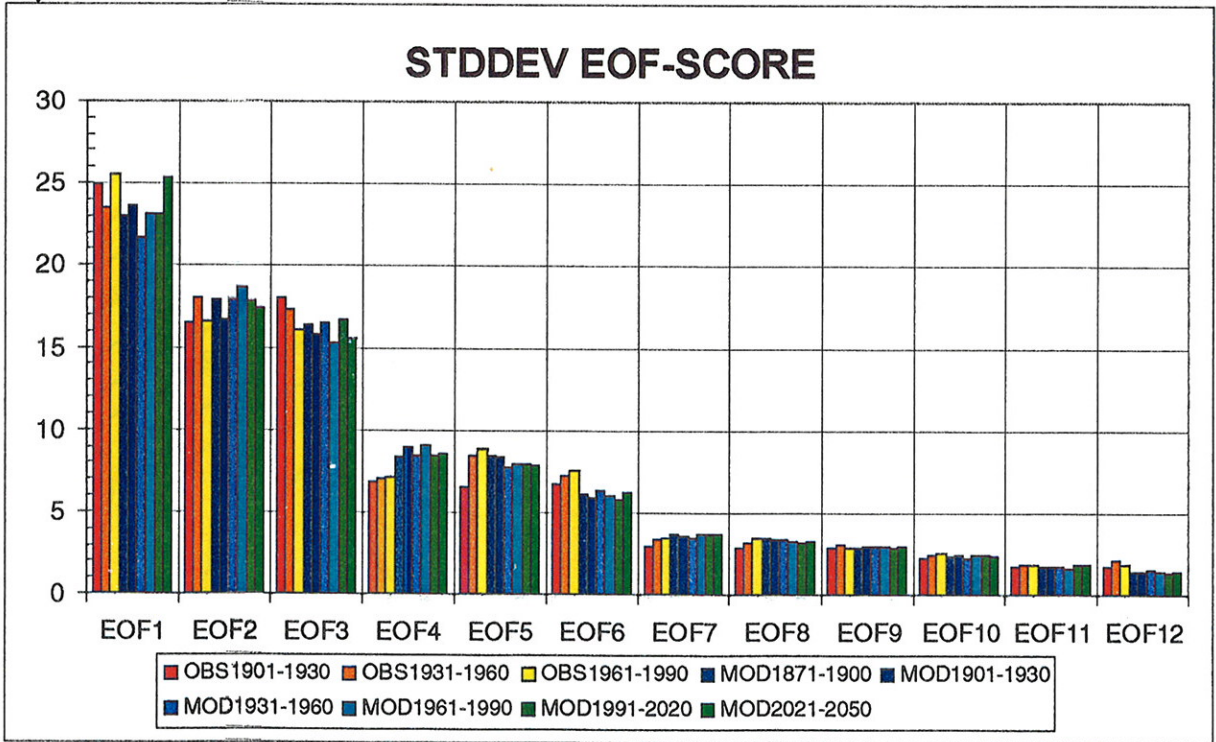


Figure 7. Mean values and standard deviations for the scores associated with the first 12 common EOFs deduced from the SLP field. Values are given for consecutive 30-year periods of observed (red/yellow bars) or GSDIO modelled (blue/green bars) temperatures.

One might expect that this bias in the modelled SLP-fields should lead to a systematic underestimation of winter temperatures. This was not seen in the present analysis, however, local ground inversions (which cannot be reproduced in the smooth model topography) may to some extent compensate for this.

The third EOF score is at average positive for observations and negative in the model (Figure 7a), which implies that the model at average has a too weak southerly (or too strong northerly) wind-field over Norway and Svalbard. The fourth EOF score, at the other hand, is at average negative for observations and positive in the model. This implies a too strong south- to south-westerly wind-anomaly over southern Norway, and a somewhat too strong south- to south-easterly wind-anomaly over northern Norway and Svalbard. The differences between modelled and observed EOF scores connected to the other EOFs are smaller, and in most cases, less systematic.

Though there are some systematic differences between the mean values of modelled and observed EOF scores, the variation around the averages seems to be realistic (Figure 7b). EOF 4 accounts for slightly more of the variance in the model than it does in reality, while it is the other way around for EOF 6. For the rest of the EOFs however, the standard deviations of the scores based on observations and model results are very similar.

4.2 Control vs. future SLP-fields

The successive 30-year averages and standard deviations of the EOF-scores (Figure 7) give an impression of eventual time trends in observed and/or modelled SLP-fields. Concerning standard deviations, no obvious trends are found. Concerning mean values, on the other hand, the model results show a clear negative trend in the scores of the first EOF, implying a strengthening of the westerly wind field over Norway (cf. Figure 6). The model shows a reduction already from 1931-1960 to 1961-1990, and a further reduction through the two following 30-year periods. It is thus suggested that the climate signal connected to the combined effect of increased concentrations of greenhouse gases and sulphur aerosols, include an increased intensity of the westerlies over Norway. Also in observations, we find a reduction (increased negative value) of the average first EOF score from 1931-1960 to 1961-1990. This seems to support the model results. However, note that the bias in the scores of the first EOF still exceeds the modelled change. A relevant question is thus: Is it reasonable to expect a further strengthening of the westerlies (as the model shows) when we in reality are starting out with a westerly wind-field that at average is stronger than the one the model produces? The question is highly relevant, as methods for creating climate change scenarios that are based on direct translation of differences between the models' control and future climate, in principle are making such assumptions.

5. Comparison of connections between SLP-field and temperature

Zorita and von Storch (1997) investigated the skills of the ECHAM1 and ECHAM3 models to reproduce the observed connection between the North Atlantic SLP field and winter temperatures in Scandinavia.

Benestad (2000a) similarly investigated the skill of ECHAM4/OPYC3 to reproduce the observed connection between the NAO index and Norwegian winter temperatures. In this present section the skill of the ECHAM4/OPYC3 model to reproduce the observed connections between the SLP field and temperatures in different parts of Norway will be investigated more in detail.

Hanssen-Bauer (1999) and Hanssen-Bauer and Førland (2000) used stepwise multiple regression analysis to connect the EOFs from the SLP field to standardised temperature series from the 6 Norwegian

Table 3 a). Correlation coefficients, January temperature vs. SLP regression model

Region or Grid-point →		Region 1, grid-point p1	Region 2n, grid-point p2n	Region 3, grid-point p3	Region 4s, grid-point p4s	Region 5, grid-point p5	Region 6, grid-point p6	Region S, grid-point pS
Data ↓ period ↓								
obs	1901-1960	0.83	0.85	0.84	0.84	0.79	0.65	0.78
	1961-1997	0.86	0.86	0.84	0.88	0.87	0.63	0.62
gsdio	1871-1900	0.86	0.82	0.82	0.78	0.75	0.64	0.55
	1901-1930	0.87	0.89	0.88	0.79	0.74	0.52	0.73
	1931-1960	0.71	0.69	0.80	0.68	0.55	0.21	0.46
	1961-1990	0.85	0.82	0.86	0.77	0.68	0.50	0.75
	1991-2020	0.83	0.80	0.84	0.83	0.80	0.73	0.56
	2021-2050	0.78	0.82	0.85	0.77	0.71	0.75	0.64

Table 3 b). Correlation coefficients, July temperature vs. SLP regression model

Region or Grid-point →		Region 1, grid-point p1	Region 2n, grid-point p2n	Region 3, grid-point p3	Region 4s, grid-point p4s	Region 5, grid-point p5	Region 6, grid-point p6	Region S, grid-point pS
Data ↓ period ↓								
obs	1901-1960	0.82	0.81	0.82	0.84	0.84	0.75	0.66
	1961-1997	0.78	0.79	0.78	0.77	0.76	0.61	0.59
gsdio	1871-1900	0.64	0.59	0.71	0.72	0.80	0.54	0.60
	1901-1930	0.61	0.35	0.66	0.74	0.75	0.36	0.55
	1931-1960	0.56	0.64	0.65	0.57	0.70	0.30	0.37
	1961-1990	0.55	0.55	0.59	0.61	0.72	0.47	0.33
	1991-2020	0.63	0.58	0.72	0.68	0.75	0.56	0.58
	2021-2050	0.66	0.54	0.77	0.71	0.77	0.55	0.34

temperature regions shown in Figure 1. Similar connections were now developed between the 12 first common EOFs and standardised temperatures from the 6 Norwegian regions and Svalbard, based upon observations during the period 1901-1960 (training period). Models were developed for January and July (see Appendix), and applied on SLP-fields observed during the period 1961-1997 (validation period), and on the SLP-fields resulting from the GSDIO integration for the period 1871-2050. Correlation coefficients between observed regional temperatures and the results from the regression models were calculated for the training period and the validation period. Similarly, correlation coefficients were calculated between the GSDIO grid-point temperatures and results from the regression models for different 30-year periods. In January (Table 3 a), the correlation coefficients for the GSDIO temperatures are, in most cases, similar to those found from observed temperatures. Exceptions are found for the model period 1931-1960, where the correlation coefficients are lower, especially at northern grid-points. This is mainly caused by very low temperatures in 1932 and 1933, when the sea-ice edge in the model probably was unrealistically far west and south (see section 3.2). One may conclude that the GSDIO integration of ECHAM4/OPYC3 very well takes care of the observed connection between the atmospheric circulation and the Norwegian winter temperatures. In July (Table 3 b) the correlation between temperatures and the results from the regression models are in most cases lower for the GSDIO series than for the observed series. Still, the correlation coefficients are clearly significant, thus the model evidently reproduces some of the observed connections also during summer.

The correlation coefficients between the GSDIO temperatures and the results from the regression models vary substantially from one 30-year period to another (which is also the case for observed temperatures though it is not shown here). However, the results in table 3 show no systematic changes in the correlation coefficients. Thus the present results give no reason to suspect that the connections between atmospheric circulation and temperatures in Norway will change.

An interesting question is if, or to what degree, the temperature trends which the GSDIO-integration produce in Norway and at Svalbard may be attributed to the established connections between the SLP field and the temperature. The January and July series of grid-point temperatures from p1, p2n, p3, p4s, p5, p6 and pS were compared to the regional series achieved by the regression model multiplied by the 1961-1990 standard deviation of the current grid-point. In January, the regression models gave temperature increases of between 1/3 and 2/3 of the warming predicted directly by the GSDIO integration for grid-points at the Norwegian mainland (Figure 8a). The temperature increases resulting from the regression models are mainly caused by the fact that an intensified south-westerly circulation brings relatively mild air-masses in over Norway during winter. At Svalbard, the contribution from the regression model was, relatively speaking, much lower, probably because much of the warming in the Arctic during winter is connected to reduced sea ice cover, which leads to strong (and non-linear) positive feedback mechanisms for the air temperature. In summer, the circulation based regression models give no contribution at all to the warming (Figure 8b).

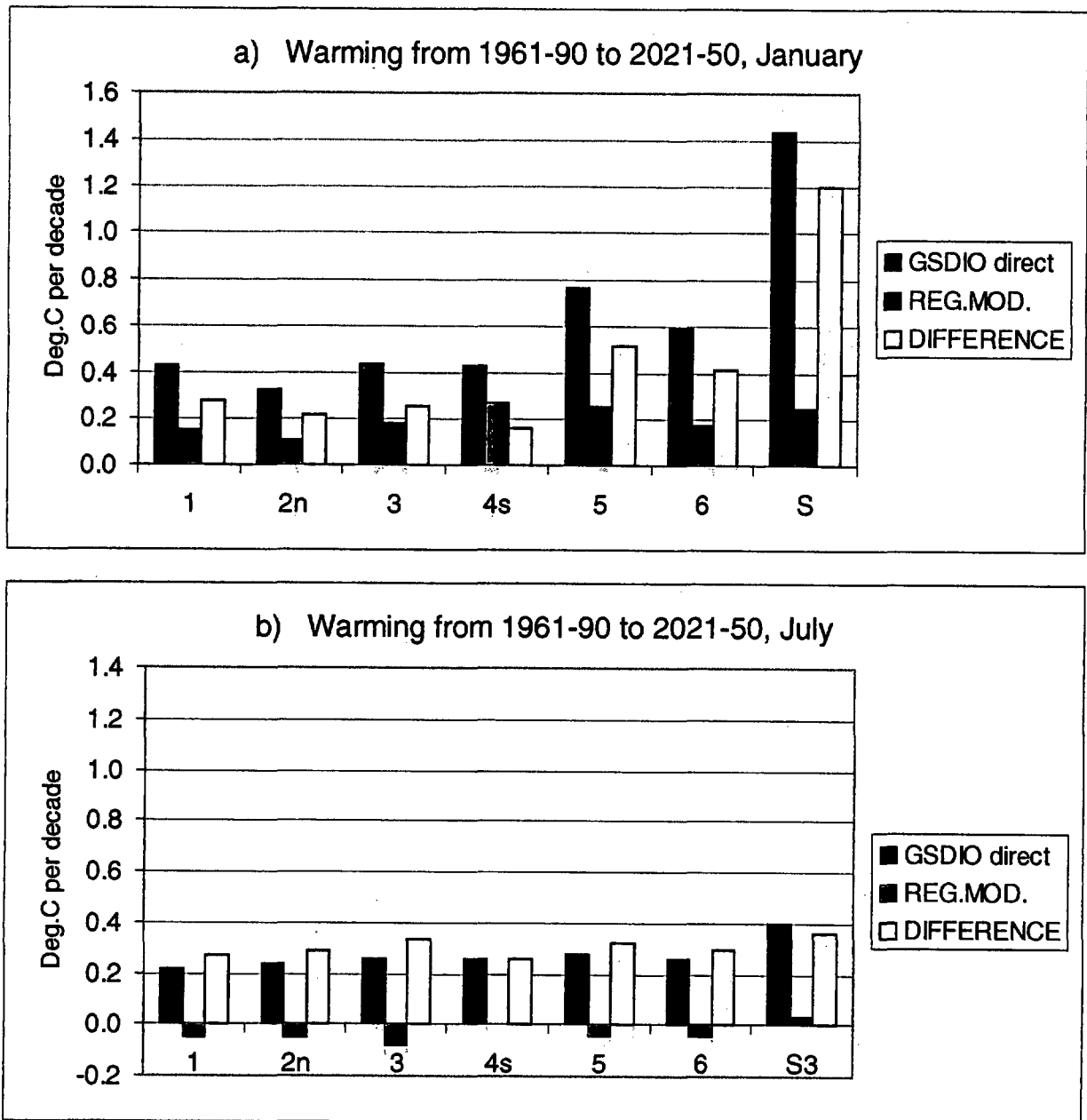


Figure 8. Temperature trends in different grid-points according to the GSDIO integration in January (upper panel) and July (lower panel). Blue bars show trends directly from the model. Red bars show trends in temperatures calculated from the regression model, using SLP fields from the GSDIO as input. Ivory bars show the difference.

One might expect this result, as an intensified westerly circulation rather brings relatively chilly air-masses in over Norway in summer. Thus, even though the warming predicted by the GSDIO integration is larger in January than in July, this is not in general true for the part of the warming which cannot be explained by the circulation based regression models. The differences between the temperature trends found directly from the GSDIO integration and those found from the regression models can be caused by non-linear effects, which are not taken care of by the linear models, or they can be caused by warming which is directly connected to changes in the climate forcing.

6. Conclusions

The GSDIO grid-point temperatures over Norway and Svalbard during the period 1871-1990 are in most cases found to be realistic, whenever it is possible to find stations with similar altitude and distance from the coast. Some outliers are found during the winter- and spring-months 1931-32 and 1932-33 at grid-points close to the northern coast of Norway. These are probably caused by unrealistically harsh sea-ice conditions. Except from this, most differences between modelled and observed temperatures may be explained by differences between grid-points and stations concerning altitude, influence of marine air-masses, or local topography.

The GSDIO "future climate" indicates an annual mean warming of 0.2 - 0.5 °C/decade in the Norwegian grid-points, and 0.8 °C/decade in the Svalbard grid-point up to 2050. The warming is at maximum in winter. It is larger in the inland than at the coast, and it increases with latitude.

The GSDIO "control climate" SLP fields give at average a somewhat too weak westerly wind-field over Norway. The GSDIO "future climate" indicates an increase in the westerly wind component in this area. Observations from the later decades show an increase in the westerly field of the same magnitude that is found in the GSDIO results during the same period. An interesting question is if the predicted continuing intensification of the westerlies is realistic, taken into account that the modelled westerlies are too weak in the "control period".

The observed connections between atmospheric circulation and temperatures in Norway and at Svalbard are satisfactorily reproduced in the GSDIO integration, especially in winter. The winter warming in the GSDIO integration may partly be explained by the increase in the westerly wind component. At the Norwegian mainland, a linear regression model based on atmospheric circulation indices accounts for 1/3 to 2/3 of the warming in January. In July, the linear regression model does not account for any warming at all. The reason for this is that an intensified westerly wind field is associated with marine air-masses, which are relatively mild in winter but not in summer. The warming which is not accounted for by the linear regression model may be caused by non-linear processes including feedback mechanisms and air-sea-ice interactions, or it may be directly connected to changes in the climate forcing.

References

- Benestad, R., 1998: Description and evaluation of the predictor data sets used for statistical downscaling in the Reg Clim project. DNMI-KLIMA 24/98, 36pp
- Benestad, R., 1999a: Conversion and quality control of the ECHAM4/OPYC3 GSDIO data to the netCDF format and a brief introduction to Ferret. KLIMA 27/99, 31pp
- Benestad, R., 1999b: Evaluation of the common EOF approach in linear Empirical Downscaling of Future ECHAM4/OPYC3 GSDIO Climate Scenarios, DNMI, Klima, 35/99.
- Benestad, R., 2000a: The cause of warming over Norway in the ECHAM4/OPYC3 GHG integration. Submitted to *Int. J. Climatol.*
- Benestad, R., 2000b: Future ECHAM4/OPYC3 GSDIO Climate Scenarios for Norway based on linear empirical downscaling and inferred directly from AOGCM results. DNMI-KLIMA , in progress.
- Benestad, R., I. Hanssen-Bauer, I., E.J.Førland, O.E. Tveito and K. Iden, 1999: Evaluation of monthly mean data fields from the ECHAM4/OPYC3 control integration. DNMI-KLIMA 14/99, pp
- Hanssen-Bauer, I. and P.Ø. Nordli 1998: Annual and seasonal temperature variations in Norway 1876-1997. DNMI-KLIMA 25/98, 29pp.
- Hanssen-Bauer, I. 1999: Downscaling of temperature and precipitation in Norway based upon multiple regression of principal components of the SLP field. DNMI-KLIMA 21/99
- Hanssen-Bauer, I. and E.J.Førland 2000: Temperature and precipitation variations in Norway and their links to atmospheric circulation. Accepted by *Int.J. Climatol.*
- Iversen, T., E.J.Førland, L.P.Røed and F. Stordal, 1997: Regional Climate Under Global Warming. Project Description. 75 pp. NILU, P.O.Box 100, N-2007 Kjeller, Norway, 75pp.
- Machenhauer, B., M. Windelband, M. Botzet, J.H. Christensen, M. Déqué, R. G. Jones, P. M. Ruti and G. Visconti, 1998: Validation and analysis of regional present-day climate and climate change simulations over Europe. MPI Rep. 275, Max-Planck-Institut für Meteorologie, 80pp.
- SAS Institute Inc., 1988: *SAS/STAT® User's Guide, Release 6.03 Edition*. Cary, NC, 1028 pp.
- Zorita, E. and H. von Storch, 1997: A survey of statistical downscaling techniques. GKSS97/E/20, 42pp.

